Quantum Electronics **49** (4) 404–408 (2019)

LASER MEDICINE

https://doi.org/10.1070/QEL16809

Effect of laser-induced hydrodynamic dissection of biotissue in operative urology

V.P. Minaev, N.V. Minaev, V.I. Yusupov, A.M. Dymov,
N.I. Sorokin, V.Yu. Lekarev, A.Z. Vinarov, L.M. Rapoport

Abstract. **We study the effects that occur in a physiological solution when laser radiation with a wavelength of 1.94 μm and a power of 60–120 W is delivered into it through an optical fibre. It is shown that as a result of the boiling of the liquid near the fibre end, a laser-induced hydrodynamic effect can be realised, in which a two-phase jet is formed, consisting of heated water and vapour-gas bubbles propagating at a speed of ~1 m s^{-1}. This jet can be used in medicine for dissecting biological tissues when removing a bladder tumour as a single unit, for dissecting the stricture of the ureter or urethra, and for enucleation of the prostate adenoma (hyperplasia). The use of this effect allows pathological tissue to be accurately separated from the underlying layer, virtually eliminating carbonisation and the formation of viable tumour fragments, which can lead to tumour dissemination. The characteristics of a laser-induced jet, which determine the nature of its effect on biological tissues, are studied experimentally, and the optimal regimes of laser irradiation are found. It is shown that the jet parameters most effective for hydrodynamic dissection of biological tissue are implemented using a radiation power of 120 W at a distance of ~3 mm from the fibre end.**

Keywords: *fibre lasers, laser-induced superintense boiling, two-phase jet, biotissue dissection, laser radiation in urology, laser enucleation of prostate adenoma, laser removal of bladder cancer.*

1. Introduction

Endoscopic surgery using laser radiation, such as laser lithotripsy, removal of a bladder tumour as a single unit, dissection of the ureteral or urethral stricture, laser enucleation of prostate adenoma (hyperplasia), etc., are becoming more and more important in the urologist's arsenal. In Refs [1, 2], the effect of laser hydrodynamic dissection was described with various surgical interventions on soft tissues carried out in a medium of saline. This effect was discovered during operations in the Urology Clinic of Sechenov University. In contrast to the traditional effect, which occurs when the end of a laser optical fibre contacts biotissues and dissection is achieved because of the combined action of laser radiation and a hot fibre end, in the considered method the effect is due to an intense two-phase (liquid-gas) jet. Such jets are formed at superintense boiling near the end of the optical fibre, when the liquid heats up quickly as a result of the absorption of laser radiation in thin layers of a special absorbing coating at the end of the fibre or in the liquid itself [3, 4].

The use of this approach in performing a number of operations (enucleation of prostate adenoma, removal of non-muscle-invasive bladder cancer) demonstrated a number of advantages over the traditional contact approach. These include:

– the ability to control the dissection zone avoiding carbonisation and thermal shining of the impact zone that mask the zone and impede its visualisation, which allows the surgeon to carry out precision separation of the removed tissue from the underlying layer;

– reducing the probability of producing viable tumour fragments (when the bladder tumour tissue is removed as a single unit), floating in a liquid and capable of disseminating the tumour, as can occur if the integrity of the tumour is disturbed during its vapourisation;

– coagulation of the cut walls with a heated two-phase jet that can be enhanced with the help of additional radiation that penetrates deeper into the biological tissue, e.g., with a wavelength of 1.55 μm using the Urolaz apparatus.

The purpose of this work is to study the physical processes that occur when radiation introduced into a physiological solution through an optical fibre is strongly absorbed by the liquid, and to determine experimentally the conditions for laser-induced hydrodynamic dissection of biotissue with the required efficiency.

2. Materials and methods

A two-wavelength Urolaz apparatus (after re-registration, FiberLaseU1) was used as a laser source, which introduced into one operating fibre the radiation from a thulium-activated fibre laser with $\lambda = 1.94$ μm and the power up to 120 W and an erbium-activated fibre laser with $\lambda = 1.55$ μm and the power up to 15 W [1]. During operations and physical experiments, a silica-silica fibre with a core diameter of 600 μm was used. Transurethral surgery was performed endoscopically.

To study the parameters of the jet, which is formed when laser radiation enters the physiological solution, we used an experimental setup, the main part of which is shown in Fig. 1.

V.P. Minaev NTO IRE-Polus, pl. Akad. Vvedenskogo 1, stroenie 3, 141190 Fryazino, Moscow region, Russia;
e-mail: vMinaev@ntoire-polus.ru;
N.V. Minaev, V.I. Yusupov Institute of Photonic Technologies, Federal Research Centre 'Crystallography and Photonics', Russian Academy of Sciences, Pionerskaya ul. 2, 108840 Moscow, Troitsk, Russia;
e-mail: minaevn@gmail.com, iouss@yandex.ru;
A.M. Dymov, N.I. Sorokin, V.Yu. Lekarev, A.Z. Vinarov, L.M. Rapoport Institute of Urology and Human Reproductive Health, I.M. Sechenov First Moscow State Medical University (Sechenov University), Bolshaya Pirogovskaya ul. 2, stroenie 1, 119992 Moscow, Russia; e-mail: alimdv@mail.ru, nisorokin@mail.ru, lekarev_bat@mail.ru, avinarov@mail.ru, leonidrapoport@yandex.ru

Received 3 October 2018; revision received 6 December 2018
Kvantovaya Elektronika **49** (4) 404–408 (2019)
Translated by V.L. Derbov

The used cuvette was 12.5 × 2.3 × 4.1 cm in size and was filled with saline to a level of 3.5 cm during the experiment. The initial temperature of the solution was 24 °C. The shadow picture of the processes occurring in the cuvette near the output end of the optical fibre was recorded using a Fastcam SA3 high-speed camera (Photron, USA) at a shutter speed of 1/10000 s, a frequency of 3800 frames s^{-1} and illumination with white or red light.

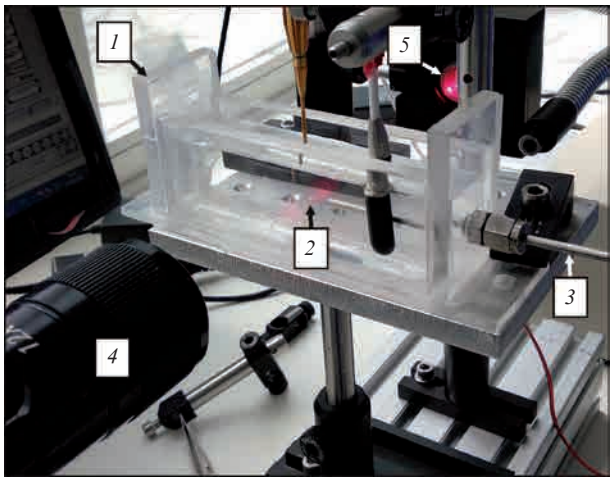

Figure 1. Main part of the experimental setup for the study of laser-induced hydrodynamic processes near the end of the laser fibre: (*1*) cuvette with saline; (*2*) distal end of a fibre with a core diameter of 600 μm; (*3*) optical fibre guide; (*4*) high-speed camera; (*5*) illuminator.

During the operations described in [1, 2], the effect of laser-induced hydrodynamic dissection of biotissue was observed during enucleation of prostatic hyperplasia with repetitively pulsed radiation with a wavelength of 1.94 μm, a peak power of 120 W and an average radiation power of 60 W. The energy of laser pulses with a duration of 12 ms was 1.4 J. The same effect was observed when a bladder tumour was removed using an average radiation power of 10 W. In this case, the peak power was also 120 W, and the impact was implemented using pulses with an energy of 1 J and a repetition rate of 10 Hz. At the same time, it was not possible to realise the effect of hydrodynamic dissection of biotissue using continuous radiation with a power of 60 W. In this case, tissue dissection could be carried out only by contact of the operating end of the laser fibre with biotissue.

In this regard, studies were conducted at maximum radiation power of 60 and 120 watts, as well as 80 and 100 watts.

3. Results and discussion

Figure 2a shows the sequences of frames obtained using a high-speed camera and illustrating hydrodynamic processes occurring near the operating fibre end in 5 ms after the supply of continuous laser radiation with a power of $P = 60$, 80, and 120 W. For all the studied powers during the first milliseconds, typical is the formation of a pulsating elongated vapour-gas macrobubble [area (*2*) in Fig. 2b] giving rise to a two-phase jet [area (*3*), Fig. 2b] that consists of heated water and small vapour-gas bubbles. The jet is visible in the photographs due to fluctuations of the refractive index and the presence of individual vapour-gas bubbles ranging in size from a few micrometres to several tens of micrometres. The speed of the two-phase jet front propagation increases on average with increasing laser power. From Fig. 2a, it can be seen that, at a power of $P = 120$ W, the vapour-gas region (shown as a circle) separates from the main jet and moves off the end of the fibre at a high speed. Note that the parameters of a pulsating elongated vapour-gas bubble [area (*2*) in Fig. 2b], which is formed at such intensities (about 10^4 W cm^{-2} at the end), were studied in detail in a number of papers (see, e.g., [5, 6]); however, the characteristics of the two-phase jet, into which it transforms, have practically not been studied.

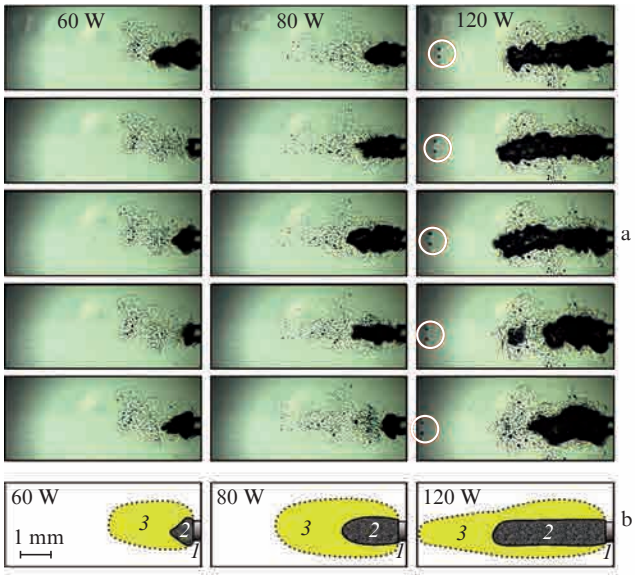

Figure 2. (a) High-speed camera images (a frame rate of 3800 s^{-1}) of laser-induced hydrodynamic processes near the operating fibre end in 5 ms after switching on the laser radiation with power $P = 60$, 80 and 120 W; (b) schematic representation of the areas near the fibre end (*1*) occupied by the vapour-gas bubble (*2*) and the heated hydrodynamic jet (*3*). The circles indicate the detached areas of the heated fluid.

Figure 3a shows the pulsations of the vapour-gas bubble length at $P = 120$ W. From Fig. 2b it follows that with increasing power P, the length of the bubble and the distance over which the two-phase jet spreads during 5 ms increases significantly. In this case, the dependence of the average bubble length L on P turns out to be almost linear (Fig. 3b): $L = 0.027P - 0.9$. Figure 3c shows the dependence of the velocity of the heated jet V at a distance of 3 mm from the fibre end face on the radiation power P. This dependence also appeared to be close to linear: $V = 0.017P - 0.9$. When the power P is increased by two times (from 60 to 120 W), the average jet velocity V increases by more than seven times (from 0.16 to 1.18 m s^{-1}). The speed of the jet propagation was determined from the movement of vapour-gas bubbles and the front of changes in the refractive index from frame to frame. The velocity V was measured in 15–20 ms after the laser radiation was switched on, when the jet front was at a significantly greater distance from the end of the laser fibre than that in Fig. 2a. As already noted, at a maximum power of $P = 120$ W, the areas of heated water periodically detach from the distal end of the vapour-gas bubble, whose velocities near the bubble reach 5 m s^{-1}.

Experiments have shown that when laser radiation is supplied, due to its good absorption by water (absorption coef-

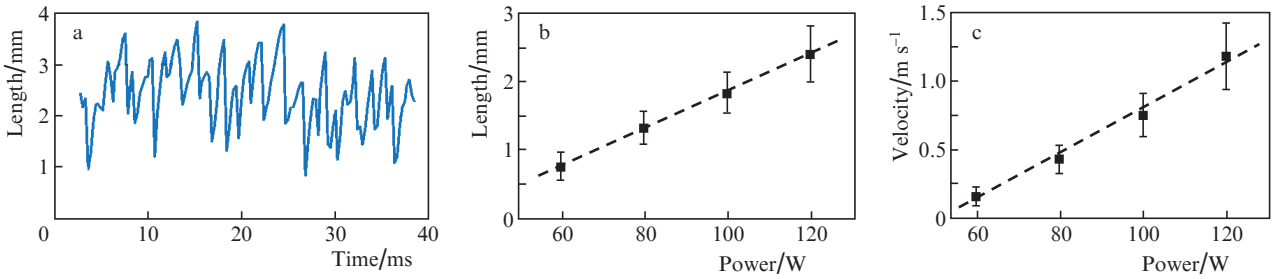

Figure 3. (a) Pulsations of the vapour-gas macrobubble length at $P = 120$ W, (b) dependence of the vapour-gas bubble length on the power P and (c) dependence of the velocity of the heated jet at a distance of 3 mm from the fibre end face on the power P. The mean values and standard deviations for the results of thirty measurements are given.

ficient is near 92 cm^{-1}) a small overheated area is produced at the fibre end, which leads to explosive boiling of water in it [3] with the formation of a pulsating vapour-gas elongated macrobubble (Fig. 2a). Since the contents of the bubble practically do not absorb radiation, it passes through it and is absorbed by the fluid at the walls of the bubble, mainly at its distal end. This phenomenon is called the 'Moses effect' referring to the biblical story, describing how the sea parted before Moses (see, e.g., [7]). This bubble passes into a two-phase jet, propagating mainly in the direction off the end of the laser fibre. Despite the constant radiation power, the boiling process is nonstationary, which leads to quasi-periodic pulsations of the length of the macrobubble (Fig. 3a). With increasing radiation power P, the bubble is increasingly elongated, and the velocity of the heated jet increases significantly. Assuming that the entire energy of the laser radiation for the first 5 ms was consumed only for heating the two-phase jet and the macrobubble formation (see Fig. 2), we estimate the average temperature increase ΔT in the jet for different P. Assuming the axial symmetry and approximating the shape of the jet [(*3*) in Fig. 2b] and the macrobubble [(*2*) in Fig. 2b] with cylinders, we obtain the following jet volumes: 2.7 ± 0.8, 4.4 ± 1.3, and 4.5 ± 1.4 mm^3 at $P = 60$, 80 and 120 W, respectively. With the values of laser energies absorbed during 5 ms taken into account, the temperature increments ΔT will be 26 ± 8, 22 ± 7 and 32 ± 9 °C, respectively. It can be seen that the increase in the temperature of the liquid in the jet weakly depends on the power P and is on average 27 ± 8 °C for all powers. Experiments have shown that with a laser power of 120 W, an elongated pulsating bubble and a heated jet, the length of which varies from ~2.5 to ~6 mm, are observed during the whole time, and for most of the time, it exceeds 3.5 mm. These values are in good agreement with the estimate of the length of the intense jet, which was obtained on the basis of the video recording of the operation and amounted to 3–5 mm [1].

Thus, there are three possible regimes of exposure to biological tissues in the medium of saline, well distinguished in frames from video recordings of operations:

I. Contact exposure to continuous radiation with a power of 60 W, when without contact it is not possible to cut the tissue. In the experiment, when the radiation power was reduced to 60 W, the average jet velocity decreased by 7 times (Fig. 3c) and, therefore, the hydrodynamic effect on the tissue, proportional to V^2, decreased by 50 times. This explains the absence of the effect of laser-induced hydrodynamic dissection of biotissue and the need for the implementation of contact action.

In this case, there is practically no water between the end of the optical fibre and the tissue, its residue and the water component of the tissue evaporate quickly, and the organic component of the tissue is heated to the carbonisation temperature. As a result, the end of the fibre and the adjacent tissue are heated to a high temperature, as evidenced by the bright shining of the contact point [(*2*) in Fig. 4a]. The jet resulting from boiling does not play a significant role, and dissection occurs because of the combined action of laser radiation and the heated fibre end, as in the case of contact in

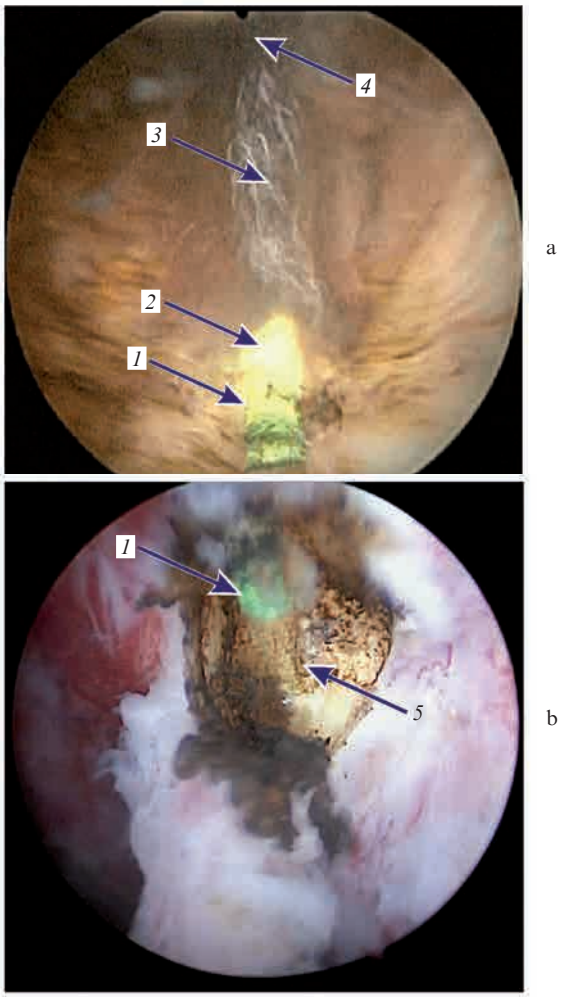

Figure 4. Formation of the incision under contact laser exposure to adenomatous tissue; (a) the radiation is switched on, (b) result of the impact: (*1*) optical fibre end; (*2*) luminous region; (*3*) vapour-gas jet; (*4*) formed incision; (*5*) carbonisation of tissue at the site of impact.

a gaseous medium. In this case, there is a noticeable carbonisation of the tissue [(*5*) in Fig. 4b], and the resulting luminescence [(*2*) in Fig. 4a] significantly masks the processes occurring at the dissection site.

II. If the dissected tissue is separated from the fibre by a distance not exceeding the length of the vapour-gas bubble [(*2*) in Fig. 5], the laser impact occurs in the 'Moses effect' regimes with laser radiation directly affecting the tissue. An example of such an effect during enucleation of prostate adenoma is shown in Fig. 5. Since radiation is absorbed mainly by the water component of the biotissue, there is a slight carbonation of the tissue in the incision area [(*3*) in Fig. 5] in places with increased absorption of light by non-aqueous components (e.g., in blood vessels). A significant portion of carbonised tissue is burned by radiation as a result of increased absorption.

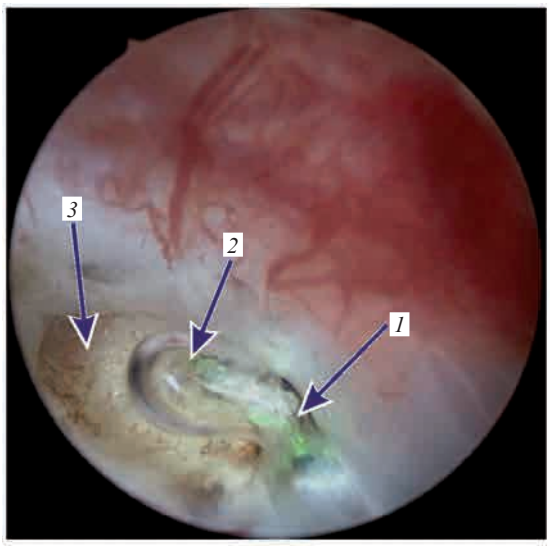

Figure 5. Impact on adenomatous tissue with the 'Moses effect': (*1*) optical fibre end; (*2*) macrobubble; (*3*) formed incision.

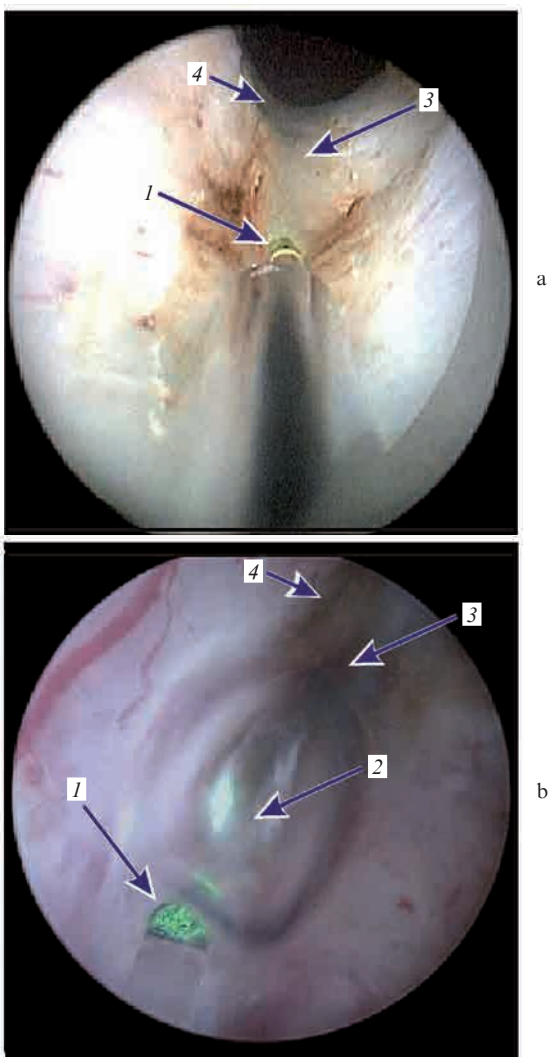

Figure 6. Laser effect on adenomatous tissue (a) in the absence of contact with tissue in the case of a collapsed macrobubble and (b) in the presence of a macrobubble: (*1*) optical fibre end; (*2*) macrobubble; (*3*) vapour-gas jet; (*4*) formed incision.

III. In the case when the biological tissue is not in contact with the bladder [(*2*) in Fig. 6b], the laser-induced hydrodynamic action of a two-phase jet [(*3*) in Fig. 6] becomes the main mechanism for the formation of the incision. Obviously, it will be most effective near the distal end of the bubble, where the jet velocity is at its maximum. In this case, carbonisation is practically not observed, and the surgeon is able to distinguish well between the abnormal and underlying tissue.

Particularly efficient operation in the regimes of laser-induced dissection is achieved in surgery aimed to remove non-muscle-invasive bladder cancer as a single unit. Figure 7 presents photographs taken in the process of resection of the bladder wall with a tumour in a single unit using laser radiation with a wavelength of 1.94 μm, a pulse power of 120 W and an average power of 10 W (1 J, 10 Hz) with contactless exposure using regimes II and III. Due to the absence of a bright shining characteristic of contact resection (regime I), the surgeon sees the muscle layer [(*2*) in Fig. 7] well, which allows delicate separation of the tumour [(*3*) in Fig. 7] as a single block that can be removed entirely. After separation of the tumour in the endoscopic image (Fig. 7c), the muscular layer is observed without traces of carbonisation.

Note that, in contrast to the vapourisation of a tumour, its removal in the laser-induced dissection regime reduces the probability of the formation of fragments of pathological tissue, which, floated in saline, can get onto the wall and cause recurrence. In addition, in this case, it is possible to obtain good material for histological studies.

4. Conclusions

When laser radiation with a wavelength of 1.94 μm and a power of ~100 W is introduced into the physiological solution through the optical fibre, a vapour-gas macrobubble is formed near the output fibre end, the content of which weakly absorbs laser radiation ('Moses effect'). At the distal end of the macrobubble an intense jet is formed consisting of hot water and vapour-gas microbubbles. With a radiation power of 120 W, the average speed of a two-phase jet near the distal end of the vapour-gas macrobubble exceeds 1 m s^{-1} and can periodically reach 5 m s^{-1}. The use of this jet allows the surgeon to carry out contactless laser-induced hydrodynamic dissection of biotissues with minimal carbonisation of the tissue at the incision site during endoscopic operations. In this

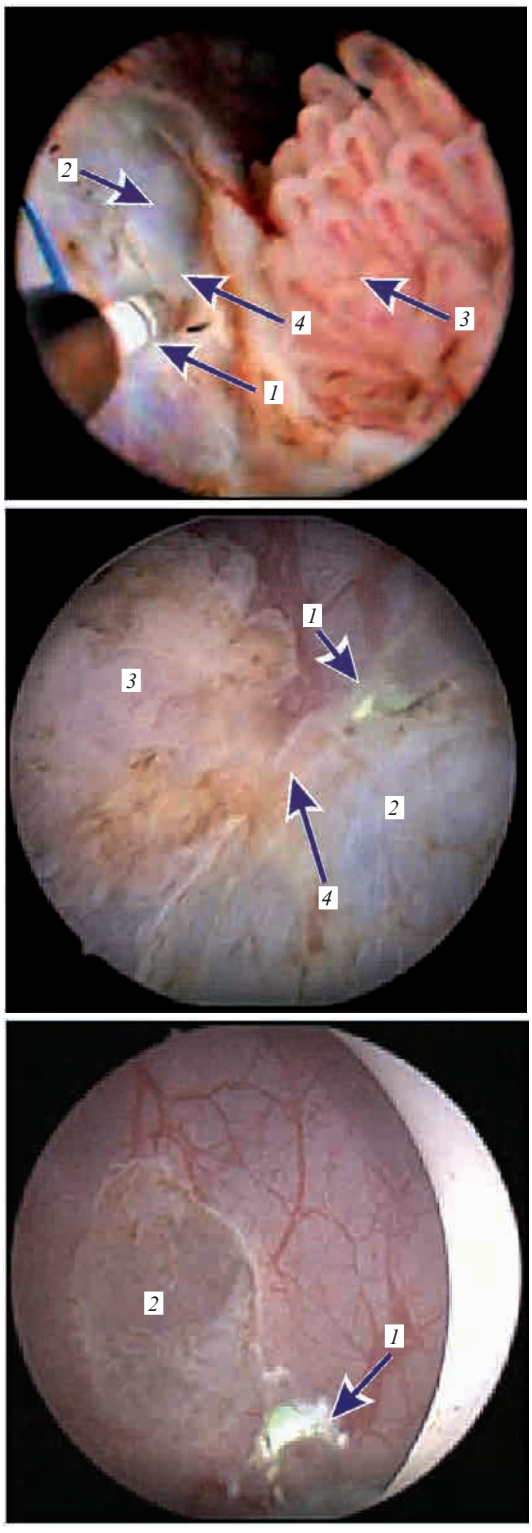

Figure 7. Laser resection of the bladder wall with a tumour as a single unit: (a, b) resection process, (c) muscle layer at the site of a removed tumour (no carbonation, no bleeding): (*1*) optical fibre end; (*2*) muscle layer under the removed tumour; (*3*) removed tumour; (*4*) tissue dissection area.

case, the doctor can clearly see the area of impact and precisely separate the removed tissue from the underlying layer. In this case, it becomes possible to drastically reduce the formation of pathological tissue fragments that can cause a relapse of the disease.

When the cw radiation power decreases to 60 W, the hydrodynamic effect on the tissue of a two-phase jet is reduced by about 50 times. In this case, the effect of laser-induced hydrodynamic dissection of the tissue is not observed, and its dissection occurs only when the operating end of the laser fibre contacts the biological tissue as a result of the combined effect of laser radiation and the heated fibre end ensuring ablation of the biological tissue. The bright shining appearing in this case prevents the surgeon from observing the area of impact, and in addition, the probability of formation of viable particles of pathological tissue increases.

Complex nonstationary processes resulting from laser-induced boiling of saline require further study.

Acknowledgements. This work was supported by the Russian Foundation for Basic Research (Grant Nos 16-02-00743 and 17-02-00832) and the Ministry of Science and Higher Education in the framework of the State Task to the Federal Research Centre 'Crystallography and Photonics' of the Russian Academy of Sciences in developing new approaches to bioablation-induced thermocavitation.

References

1. Vinarov A.Z., Dymov A.M., Sorokin N.I., et al. *Laz. Med.*, **21** (4), 50 (2017).
2. Vinarov A., Dymov A., Sorokin N., Minaev V., Lekarev V. *KnE Energy*, **3** (3), 407 (2018), DOI: https://doi.org/10.18502/ken.v3i3.2055.
3. Chudnovsky V.M., Yusupov V.I., Dydykin A.V., et al. *Quantum Electron.*, **47** (4), 361 (2017) [*Kvantovaya Elektron.*, **47** (4), 361 (2017)].
4. Chudnovsky V.M., Yusupov V.I., Zhukov S.A., Echmaev S.B., Bagratashvili V.N. *Dokl. Phys.*, **62** (4), 174 (2017) [*Dokl. Akad. Nauk,* **473** (5), 533 (2017)].
5. Hardy L.A., Kennedy J.D., Wilson C.R., Irby P.B., Fried N.M. *J. Biophoton.*, **10** (10), 1240 (2017).
6. Gonzalez D.A., Hardy L.A., Hutchens T.C., Irby P.B., Fried N.M. *Opt. Eng.*, **57** (3), 036106 (2018).
7. Elhilali M.M., Badaan S., Ibrahim A., Andonian S. *J. Endourol.*, **31** (6), 598 (2017).